Characteristics of Monolayers of Ferrocene Derivatives and Estimation of Electrical Double Layers Formed in Langmuir Films

Toshihiro KONDO,# Ramesh C. AHUJA,† Dietmar MÖBIUS,† and Masamichi FUJIHIRA*
Department of Biomolecular Engineering, Tokyo Institute of Technology, 4259, Nagatsuta, Midori-ku, Yokohama 227
†Max-Planck-Institut für Biophysikalische Chemie, D-3400 Göttingen, Germany

(Received June 11, 1993)

In order to estimate the potential difference of the electrical double layer formed in heterogeneous Sensitizer (S)/Electron Donor (D) Langmuir–Blodgett (LB) films, the surface potentials of the constituent monolayers were measured simultaneously with the π–A isotherms. The S monolayer was a mixed $[Ru(bpy)_3]^{2+}$ complex monolayer with a long alkyl fatty acid, while the D monolayer was one of three kinds of ferrocene monolayers with different signs of the hydrophilic head groups and with the same redox potential. The formation of the potential difference between the charged head group of the amphiphile and its counterion at the water-air interface was confirmed; those values were consistent with the electrical double-layer effect on the luminescent lifetime of $[Ru(bpy)_3]^{2+}$ in the S monolayer in contact with the D monolayer.

It has been pointed out that the value of the inner potential difference of the electrical double layer formed between different phases can not be measured electrochemically.[1] Thus, a direct estimation of the potential difference of the electrical double layer has attracted the attention of many electrochemists for a long time.

By making use of a heterogeneous Langmuir–Blodgett (LB) trough, which enable one to form a multilayer having more than two kinds of monolayers, the intermolecular electron transfer[2—4] and energy transfer[5] in well organized monolayer assemblies have been extensively investigated. We have studied the effects of the distances and energy gaps between the sensitizers (S) and electron donors (D) on intermolecular[6,7] and intramolecular[8] electron transfer in LB films. In the course of these investigations, we found that the inner potential differences in heterogeneous LB films are formed by the head-group charge and the counterion, and that those potential differences influence the photoinduced electron-transfer rates in various S/D LB systems.[9] If these potential differences formed in heterogeneous LB films can be estimated by any means, the effect of the electrical double layer on the photoinduced electron transfer could be discussed in a more quantitative manner.

The surface potential of a monolayer is measured as the potential difference before and after the monolayer formation on an aqueous subphase. The observed surface potential can be related to the dipole moments, due to the tail group of the amphiphilic molecules and the dipole moment or the electrical double layer between the polar head group and the aqueous subphase. Thus, the relative values of the inner-potential differences of the electrical double layers created with different signs of the head group can be estimated by comparing the surface potentials of these different monolayers. By using neutral, cationic, and aninic micelles, Fromherz and his co-workers estimated the electrical double layer and polarities by using coumarin dyes incorporated in micelles, as fluorescent probes.[10] Blinov et al.[11] have investigated the local fields in dielectric LB films by stark spectroscopic techniques, and De Schryver et al.[12] studied the relation among the ionization potential, the interfacial electric field, and the influence on the photoinduced hole transfer processes in LB films. At a symposium recently held on electrified interfaces,[13] several theoretical and experimental publications regarding electrical double layers at solid/liquid interfaces were reported.

In the present work we synthesized three kinds of ferrocene amphiphiles with different signs of their head-group charge and with the same residual part. The surface potentials of the monolayers of such three kinds of ferrocene derivatives were measured. Those values were finally compared with the results of the luminescent decay rates of the heterogeneous S/D LB systems and are discussed in terms of the effect of the electrical double layer on the energy-gap law for a photoinduced electron transfer.

Experimental

1. Materials. The $[Ru(bpy)_3]^{2+}$ amphiphilie (RuC19) was prepared and purified by methods described in the literature.[14] Three kinds of ferrocene amphiphiles (AFc, NFc, and CFc) have an anionic $-COO^-$, a nonionic $-COOCH_3$, and a cationic $-N^+(C_2H_5)_3$ head group, respectively.[9] GR grade arachidic acid (AA) from Aldrich was used without further purification. All other chemicals were the same as those described previously.[7,9]

2. Syntheses of Ferrocene Derivatives. The synthetic routes of AFc, NFc, and CFc are shown in Schemes 1 and 2. Stearoylferrocene was prepared by the Friedel–Crafts acylation with ferrocene and stearoyl chloride in the presence of $AlCl_3$.[15] NFc (methyl-6-(1′-(1-stearoyl)-ferrocenoyl)hexanoate) was prepared by the Friedel–Crafts acylation of stearoylferrocene with adipyl chloride monomethylester, which was prepared from adipic acid mono-

#Present address: Department of Chemistry, Faculty of Science, Hokkaido University, Sapporo 060.

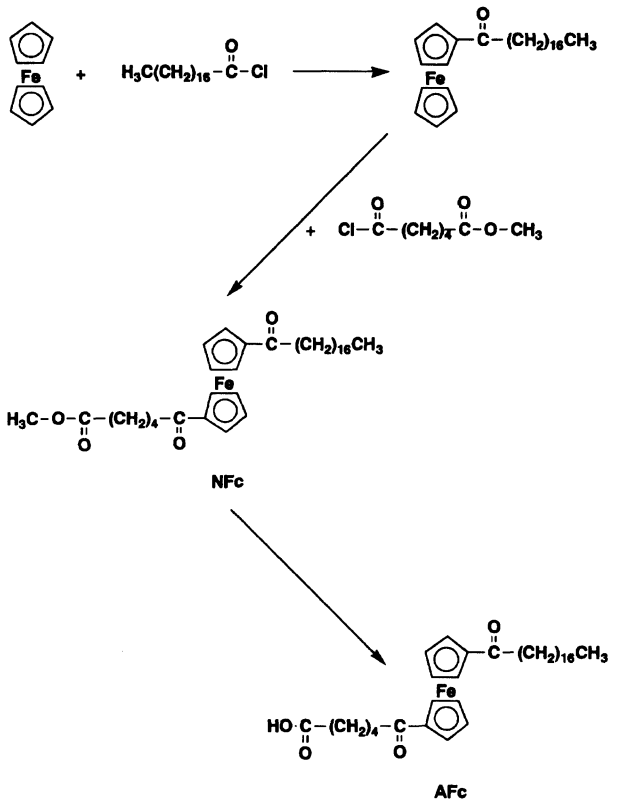

Scheme 1. Synthetic route for NFc and AFc.

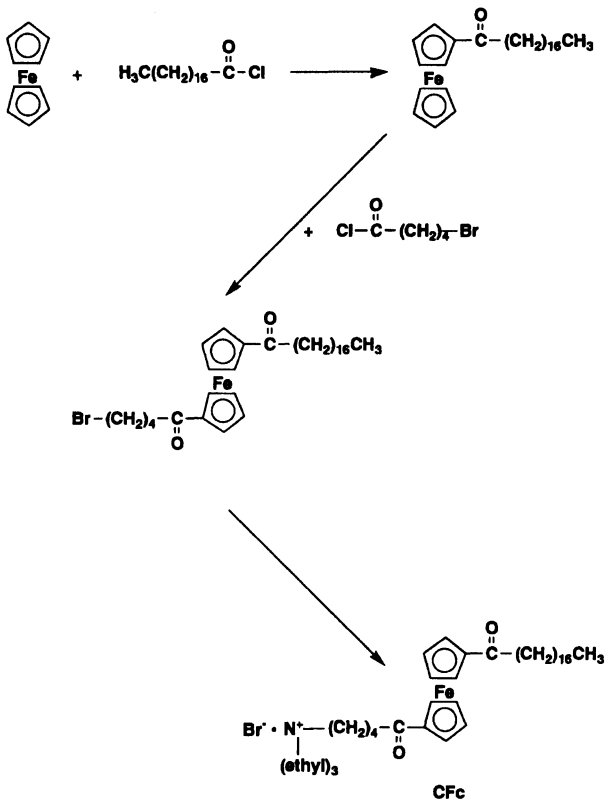

Scheme 2. Synthetic route for CFc.

methylester and excess freshly distilled thionyl chloride. The product was purified by column chromatography on silica gel with chloroform used as an eluant to yield 38.4% (10.35 g) of methyl-6-(1′-(1-stearoyl)ferrocenoyl)hexanoate. ^{1}H NMR ($CDCl_3$) δ=0.86—0.97 (t, 3H, CH_3), 1.30 (m, 30H, CH_2), 1.62—1.85 (m, 4H, CH_2), 2.38 (t, 2H, –O–C(=O)–CH_2), 2.65 (t, 4H, C(=O)–CH_2), 3.65 (s, 3H, C(=O)–O–CH_3), 4.40 (t, 4H, arom(ferrocene)), 4.70 (d, 4H, arom(ferrocene)). AFc (6-(1′-(1-stearoyl)ferrocenoyl)hexanoic acid) was prepared by alkali hydrolysis of NFc.[16] The product was purified by column chromatography on silica gel with mixtures of benzene and acetone (9:1—2:1) to yield 28% (0.14 g) of 6-(1′-(1-stearoyl)ferrocenoyl)hexanoic acid. ^{1}H NMR ($CDCl_3$) δ=0.86—0.97 (t, 3H, CH_3), 1.30 (m, 30H, CH_2), 1.62—1.85 (t, 4H, C(=O)–CH_2), 2.38 (t, 2H, –O–C(=O)–CH_2), 2.65 (t, 4H, C(=O)–CH_2), 4.40 (t, 4H, arom(ferrocene)), 4.70 (d, 4H, arom(ferrocene)). 1-Bromo-5-(1′-(1-stearoyl)ferrocenoyl)-5-on-pentene was prepared by the Friedel–Crafts acylation of stearoylferrocene with 5-bromovaleryl chloride. CFc (5-(1′-(1-stearoyl(ferrocenoyl)-5-on-pentyltriethylammonium bromide) was prepared by quaternization of 1-bromo-5-(1′-(1-stearoyl)ferrocenoyl)-5-on-pentene with triethyl amine.[17] Anal. Calcd for $C_{39}H_{66}O_2NBrFe$(716.71): C, 65.36; H, 9.28; N, 1.95; Br, 11.14%. Found: C, 65.45; H, 9.18; N, 1.87; Br, 11.53%.

3. Preparations and Measurements of the Monolayers. The monolayers were prepared at the water/air interface of a rectangular Teflon trough with inner dimensions of 56×18 cm^2 and a depth of 1 cm, that was enclosed in a tight box and thermostated. The surface pressure was measured by a filter-paper Wilhelmy balance. The surface potential was measured with a vibrating-plate condenser. The principle of the potential measurement is given in Fig. 1.[18] Deionized water filtered by a Milli-Q system was used as a subphase for monolayer preparation. For monolayers, the $[Ru(bpy)_3]^{2+}$ derivative was mixed with AA at a molar ratio of 1:2 or used by itself, while the ferrocene derivatives were used by themselves. The surface pressures and potentials were measured at 15 °C, mostly on pure water; for AFc, however, they were also measured on 0.3 mM $CaCl_2$ and 0.15 mM $NaHCO_3$ (1 M≡1 mol dm^{-3}) ; for mixed $[Ru(bpy)_3]^{2+}$ and NFc monolayers, they were also measured on 0.05 mM $NaHCO_3$. All of the sample preparations and measurements were carried out in the dark to avoid photooxidation of the films.[19]

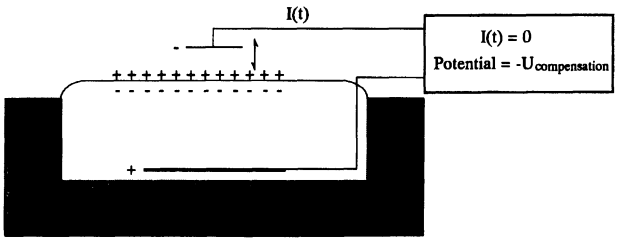

Fig. 1. Change in the surface potential due to the formation of a monolayer (ΔV) measured by the vibrating-plate condenser method: One platinum electrode is put into an aqueous subphase; the second electrode vibrates in air at a distance of about 2 mm from the interface. The current due to periodical capacitance changes is compensated. The air electrode is grounded.[18]

Results and Discussion

The surface pressure–area (π–A) and surface potential–area (ΔV–A) isotherms of the monolayers are shown in Fig. 2. As shown in the π–A curves in Figs. 2a, 2b, and 2c, the surface pressure of the RuC19 pure monolayer, that of the mixed monolayer of RuC19 and AA with a molar ratio of 1 : 2, and that of the pure monolayer of stearic acid (SA) start to increase from a mean area of 1.05, 0.50, and 0.24 nm^2 $molecule^{-1}$, respectively. Because the area per molecule of a normal carboxylic acid with a single alkyl chain is 0.20—0.24 nm^2 $molecule^{-1}$,[20] and both AA and SA have long alkyl chains and carboxyl head groups, we can assume here that the mean area of the AA monolayer is the same as that of the SA monolayer. Since the mean areas of pure RuC19 and pure AA monolayers are 1.05 and 0.24 nm^2 $molecule^{-1}$, respectively, the mean area of the mixed monolayer of RuC19 and AA with a molar ratio of 1 : 2 would be 0.51 nm^2 $molecule^{-1}$ if the mixed film is ideal, i. e. $(1.05+0.24\times2)/3=0.51$ nm^2 $molecule^{-1}$. Although the observed mean area of 0.50 nm^2 $molecule^{-1}$ was in a good agreement with this value, the ideality of the mixed film may be superficial, because the components interact strongly and form stable neutralized ion pairs, as described later.

The change in the surface potentials due to the formation of a monolayer (ΔV) is proportional to the change in the normal component of the dipole density ($n\cdot\mu$), as given by the Helmholtz equation,

$$\Delta V = n\mu/\varepsilon_0 \tag{1}$$

or

$$\mu = \varepsilon_0 \Delta V A, \tag{2}$$

where the number of molecules per unit area (n) is related to the mean area per molecule (A) by $n=1/A$ and ε_0 is the permittivity of the vacuum. We can give the total effective dipole moment(μ) as

$$\mu = \mu_\alpha + \mu_\omega, \tag{3}$$

where μ_α is the effective dipole moment due to the polar monolayer head group region and μ_ω is that of the hydrophobic end.[18]

The surface–potential data of the condensed monolayers are listed in Table 1. Vogel and Möbius analyzed the local surface potentials (local electric dipole moments) by separating the contributions of the hydrophobic and hydrophilic monolayer interfaces described above.[18] From their analysis, the dipole moments of the CH_3-group (μ_{CH_3}) and the hydrated carboxylato group (μ_{COO^-}) are 0.35 D and −0.20 D (1 D= 3.3356×10^{-30} m), respectively. Hence, the total dipole moment of the SA monolayer is 0.15 D, and the calculated surface potential from its mean area is 285 mV by Eqs. 3 and 2, respectively. This result is very close to the present observation of +280 mV. However, in spite of the positive sign of the divalent cation head group, ΔV for the pure RuC19 monolayer is less than that for SA with the carboxylate anion. On the contrary, ΔV has a much more positive value for a cationic CFc monolayer, as we would expect. As shown in Fig. 3, in the pure RuC19 monolayer, it is expected that the head group of RuC19 occupies an area of 1.05 nm^2 $molecule^{-1}$, and the space over the head group is too widely open for the two straight alkyl chains to fill the space; consequently, the space must be filled with the folded alkyl chains. In other words, if the two alkyl chains stand normal to the air–water interface in the extended straight chain form, they would occupy 40% of hydrophobic region of the pure RuC19 monolayer, and the residual 60% would be free space. Thus, in the hydrophobic region filled with the folded alkyl chains, the positive dipole moments of the tail groups ($-CH_3$) are directed in random orientation. The idea that the contribution of this large positive dipole to the surface potential is reduced by random orientation rationalizes the small surface potential observed in the pure RuC19 monolayer. Still, in the surface potentials of the ferrocene derivatives discussed below, the effect of the reduction in the μ_ω by the random orientation due to the somewhat large molecular areas may not be negligible, but is expected to be smaller than that for the pure RuC19 monolayer.

The mean areas and the surface potentials of AFc, NFc, and CFc, are 0.44, 0.44, and 0.47 nm^2 $molecule^{-1}$ and +360, +380, and +720 mV, respectively (Table 1). These mean areas of ferrocene amphiphiles are consistent with the calculated value of a ferrocene ring, and with the reported value of the cross-sectional area of the ferrocene moiety.[21] These mean areas are almost the same as that for the mixed monolayer of 0.50 nm^2 $molecule^{-1}$. Even if the average area per alkyl chain is taken into account for the mixed monolayer, i. e. $1.50/4=0.375$ nm^2 $molecule^{-1}$, the average area is also almost comparable to those of the ferrocene amphiphiles. Therefore, among these four monolayers, the contribution of μ_ω can be concluded to be roughly comparable. In view of these considerations, the order of the surface potentials, CFc > 1 : 2 mixed > NFc > AFc monolayers, can be attributed to the contribution of the head dipole moments (μ_α). Namely, for the CFc monolayer, the value of the surface potential is the most positive among them, because of its cationic head group, $-N^+(C_2H_5)_3$. In previous studies[9] we assumed that the head group charges of the mixed monolayer are neutralized by mixing the anionic AA to divalent cationic $[Ru(bpy)_3]^{2+}$ with a molar ratio of 2 : 1. Since ΔV for the mixed monolayer gives a medium value between those for a cationic CFc and an anionic AFc, one can assume that the head groups of the 1 : 2 mixed monolayer are neutralized with each other and, as a whole, the head group of the 1 : 2 ion pair can be regarded as being a nonionic one. In contrast, the value of ΔV for NFc is

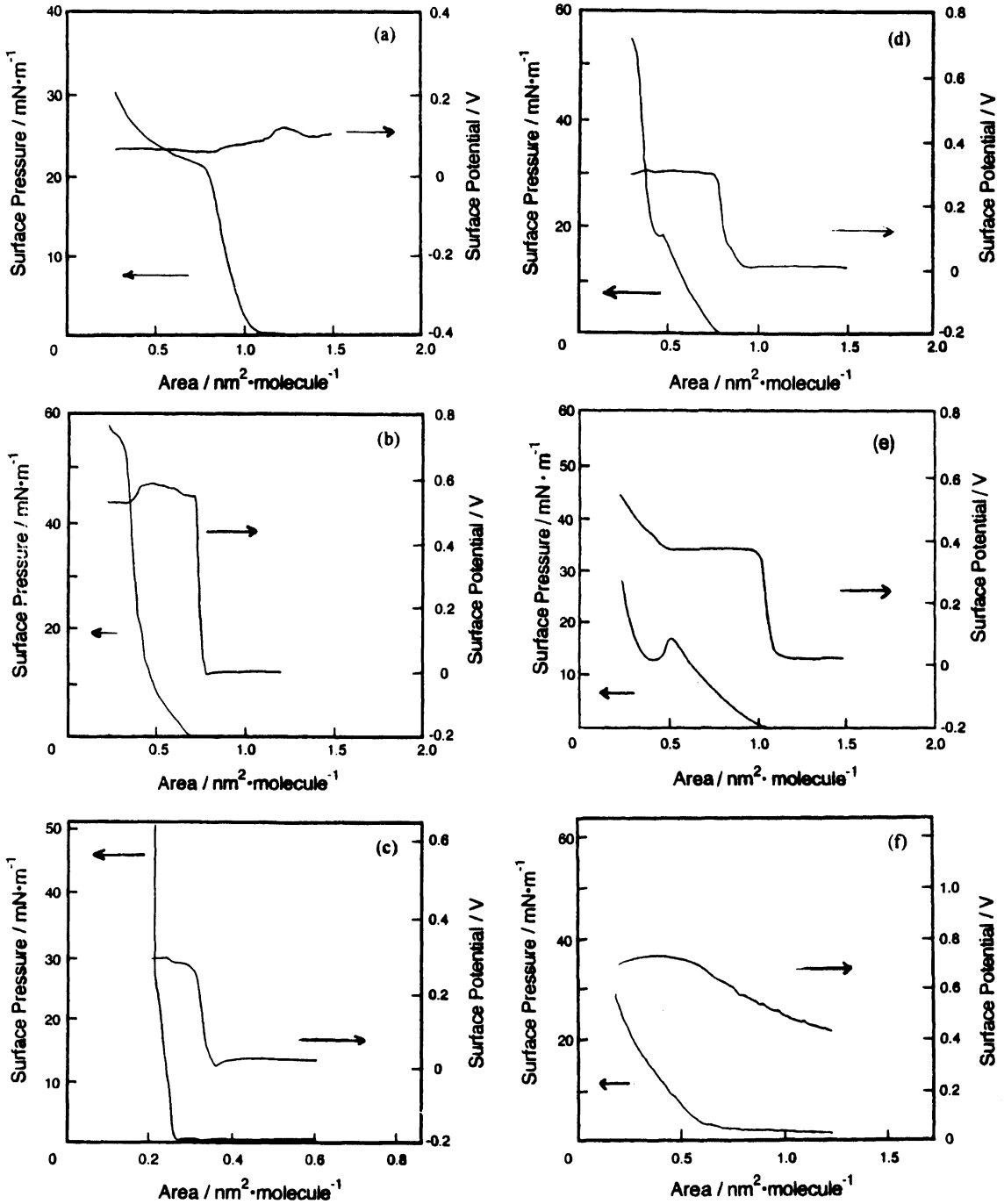

Fig. 2. Surface pressure (π)–area and surface potential (ΔV)–area isotherms of the (a) a pure RuC19 monolayer on H_2O, (b) a mixed RuC19 : AA=1 : 2 monolayer on 0.15 mM $NaHCO_3$, (c) SA monolayer on H_2O, (d) AFc monolayer on 0.3 mM $CaCl_2$+0.15 mM $NaHCO_3$, (e) NFc monolayer on 0.15 mM $NaHCO_3$, and (f) CFc monolayer on H_2O.

closed to that for AFc, although NFc has a nonionic head group, $-COOCH_3$. This result is, however, consistent with the reported dipole moment of the methoxycarbonyl group.[18] It is therefore not necessarily true that the neutral head group does not have a negligible small μ_α.

Previously, when the energy-gap dependence of the electron transfer rate in S(RuC19)/D(AFc, NFc, or CFc) heterogeneous LB films was studied, an efficient photoinduced electron transfer quenching occurred, even in S/D LB films in which the reaction was expected to be up-hill energetics. In the luminescent lifetime measurements of these S/D LB systems, the order of longness of the luminescence lifetimes of the $[Ru(bpy)_3]^{2+}$ moiety in the heterogeneous S/D LB films was on the order of the used D monolayers of CFc> NFc>AFc.[9] The most important and intrinsic factor in LB films which affect the relative energy levels between

Table 1. Molecular Mean Areas and Surface Potentials of Various Monolayers

Monolayers	Hydrophilic groups	Subphases	Molecular mean areas A/nm^2 molecule^{-1}	Surface potentials ΔV/mV
Pure RuC19	$[Ru(bpy)_3]^{2+}$	H_2O	1.05	100
RuC19 : AA=1 : 2	$[Ru(bpy)_3]^{2+}$+–COO^-	0.15 mM $NaHCO_3$	0.50	570
SA	$-COO^-$	H_2O	0.24	280
AFc	$-COO^-$	0.3 mM $CaCl_2$+ 0.15 mM $NaHCO_3$	0.44	360
NFc	$-COOCH_3$	0.15 mM $NaHCO_3$	0.44	380
CFc	$-N^+(C_2H_5)_3$	H_2O	0.47	720

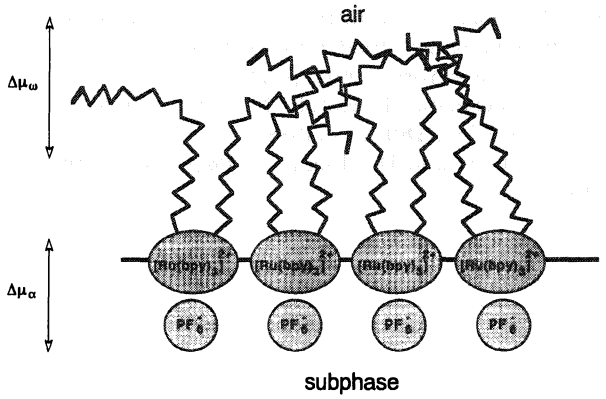

Fig. 3. Schematic structure of a pure RuC19 monolayer at the air/water interface.

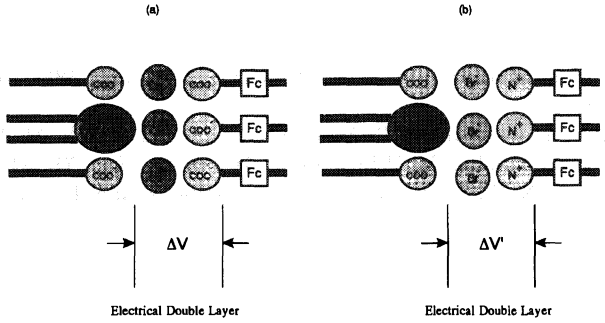

Fig. 4. The structures of S/D heterogeneous LB films and electrical double layers (EDL) created between the S and D monolayers. (a) Schematic diagram of EDL created in the S/AFc pair; (b) EDL in the S/CFc pair.

the D and S molecules may be the electrical potential differences created between the monolayers inside the LB films. As shown in Fig. 4, the region across which the electron transfer is expected to occur is the electrical double layer where the hydrophilic head groups of the RuC19 and ferrocene amphiphiles face each other. As shown in the schematic diagram of the LB structure in Figs. 4a and 4b, it seemed to be quite reasonable to assume that: i) the positive charges of $[Ru(bpy)_3]^{2+}$ are neutralized by the carboxylate anions present in the same plane in the mixed monolayer, ii) the negative charges of the head groups of AFc ($-COO^-$) are in contact with their Ca^{2+} cations, and iii) the positive charges of CFc ($-N^+(C_2H_5)_3$) in contact with Br^- counter anions. Namely, the difference in the lifetimes was interpreted in terms of the effect of the electrical double layer on the free energy of the photoinduced electron transfer in the heterogeneous LB films. The present experimental results concerning the surface potential for AFc, NFc, and CFc support the explanation mentioned above.

Although the features of π–A curves for AFc and NFc are very similar, and the values of the mean areas are the same, it is found from Brewster angle microscopy (BAM) that the stabilities of the monolayers are quite different.[22] Both π–A isotherms for AFc and NFc have one peak with a range of 10—20 mN m^{-1}. For the AFc monolayer, the monolayer is still stable after compressing beyond this peak. On the contrary, the monolayer is collapsed and crystallized after this peak for NFc. It is suggested that the hydrophilicity of the carboxylate anion is more powerful than that of the nonionic methoxycarbonyl group and stabilized the monolayer. However, for the CFc monolayer, the monolayer on the water is homogeneous. The homogeneity can be explained by the complete dissociation of the ammonium head groups, and is also consistent with the high surface potential observed before the surface pressure starts to increase.[9]

References

1) J. O'M. Bockris and A. K. N. Reddy, "Modern Electrochemistry," Plenum Press, New York (1973).
2) H. Kuhn, *Pure Appl. Chem.*, **53**, 2105 (1981).
3) D. Möbius, *Acc. Chem. Res.*, **14**, 63 (1981); *Mol. Cryst. Liq. Cryst.*, **96**, 319 (1983).
4) M. Fujihira, *Mol. Cryst. Liq. Cryst.*, **183**, 59 (1990).
5) N. Tamai, T. Yamazaki, and I. Yamazaki, *Chem. Phys. Lett.*, **147**, 25 (1988); *Thin Solid Films*, **179**, 451 (1989).
6) M. Fujihira, K. Nishiyama, and H. Yamada, *Thin Solid Films*, **132**, 77 (1985); M. Fujihira, K. Nishiyama, and K. Aoki, *Thin Solid Films*, **160**, 317 (1988).
7) T. Kondo, H. Yamada, K. Nishiyama, K. Suga, and M. Fujihira, *Thin Solid Films*, **179**, 463 (1989).
8) M. Fujihira and H. Yamada, *Thin Solid Films*, **160**, 125 (1988); M. Fujihira and M. Sakomura, *Thin Solid Films*, **179**, 471 (1989).
9) T. Kondo and M. Fujihira, *Chem. Lett.*, **1991**, 191; T. Kondo, M. Yanagisawa, and M. Fujihira, *Electrochim.*

Acta, **36**, 1793 (1991).
10) P. Fromherz, *Biochim. Biophys. Acta*, **323**, 326 (1973); M. S. Fernández and P. Fromherz, *J. Phys. Chem.*, **81**, 1755 (1977).
11) L. M. Blinov, S. P. Palto, and S. G. Yudin, *J. Mol. Electronics*, **5**, 45 (1989).
12) M. V. Anweraer, B. Verschuere, G. Biesmans, and F. C. DeSchryver, *Langmuir*, **3**, 45 (1987).
13) For example: G. M. Torrie and G. N. Patey, *Electrocim. Acta*, **36**, 1677 (1991); E. Evans and J. Ispen, *Electrochim. Acta*, **36**, 1735 (1991); D. Bratko and D. Henderson, *Electrochim. Acta*, **36**, 1761 (1991).
14) G. L. Gaines, Jr., P. E. Behnken, and S. J. Balenty, *J. Am. Chem. Soc.*, **100**, 6549 (1978); E. Borgarello, J. Kiwi, E. Pelizzetti, M. Visca, and M. Grätzel, *Nature*, **289**, 158 (1981).
15) P. J. Graham, R. V. Lindsey, G. W. Parshall, M. L. Peterson, and G. M. Whitman, *J. Am. Chem. Soc.*, **79**, 3416 (1957); N. Sugiyama, H. Suzuki, Y. Shioura, and T. Teitei, *Bull. Chem. Soc. Jpn.*, **35**, 767 (1962).
16) C. F. Allen and M. J. Kalm, *Org. Synth.*, Coll. Vol. IV, 608 (1963).
17) S. Yamaguchi, Y. Yamakawa, and T. Tsukamoto, *Rev. Polarogr.*, **17**, 145 (1971); A. B. Scott and H. V. Tartar, *J. Am. Chem. Soc.*, **65**, 692 (1943).
18) V. Vogel and D. Möbius, *Thin Solid Films*, **132**, 205 (1985); *Thin Solid Films*, **159**, 73 (1988); *J. Colloid Interface Sci.*, **126**, 408 (1988).
19) T. Kondo and M. Fujihira, *Kobunshi Ronbunshu*, **47**, 921 (1990); M. Fujihira, M. Yanagisawa, T. Kondo, and K. Suga, *Thin Solid Films*, **210/211**, 265 (1992).
20) A. Ulman, "An Introduction to Ultrathin Organic Films from Langmuir–Blodgett to Self-Assembly," Academic Press, Inc., New York (1991), p. 115.
21) H. Nakahara, T. Katoh, M. Sato, and K. Fukuda, *Thin Solid Films*, **160**, 153 (1988).
22) D. Hönig and D. Möbius, *J. Phys. Chem.*, **95**, 4590 (1991).